Available online at www.sciencedirect.com
SCIENCE DIRECT®
PERGAMON
Applied Geochemistry 18 (2003) 1531–1540
Applied Geochemistry
www.elsevier.com/locate/apgeochem

Dissolution kinetics of schwertmannite and ferrihydrite in oxidized mine samples and their detection by differential X-ray diffraction (DXRD)

Bernhard Dold*,[1]

Earth Sciences Department, University of Geneva, Rue des Maraîchers 13, 1211 Genève 4, Switzerland

Received 1 March 2002; accepted 30 December 2002
Editorial handling by B. Kimball

Abstract

A dissolution test with 9 natural and synthetic schwertmannite and ferrihydrite samples was performed by reaction with 0.2 M ammonium oxalate at pH 3.0 in the dark. The method was coupled with differential X-ray diffraction (DXRD) to successfully detect schwertmannite at low concentrations in oxidized mine tailings. Rapid dissolution was observed for all schwertmannites (> 94% in 60 min) and natural 2-line ferrihydrites (> 85% in 60 min); however, synthetic 2-line and 6-line ferrihydrite dissolved slower (42 and 16% after 60 min, respectively). The results showed that it was not possible to distinguish between natural schwertmannites and ferrihydrites on the basis of their dissolution kinetics. Modeling of the schwertmannite dissolution curves, examinations of mineral shape by scanning electron microscopy, and Fe/S mole ratios of the dissolved fractions indicated that two different schwertmannite particle morphologies (spherical and web-like) occurred. Collapse of spherical (sea-urchin) schwertmannite aggregates seemed to control the dissolution kinetics according to a shrinking core model. In the case of web-like schwertmannite, dissolution could be modeled with a simple first order equation, and structural SO_4^{2-} may have affected the dissolution kinetics. No relationship was found between ferrihydrite particle shape and dissolution behavior in acid NH_4-oxalate. A 1-h extraction with 0.2 M NH_4-oxalate at pH 3.0 in the dark should be adequate to dissolve schwertmannite and natural 2-line ferrihydrite in most samples. In some cases, a fraction of secondary jarosite or goethite may also be dissolved, although at a slower rate. If only schwertmannite is of interest (e.g., determination by DXRD), a 15 min attack should be used to increase selectivity. A truly selective leach of schwertmannite and ferrihydrite should be based on dissolution tests, as a broad variety of dissolution kinetics can be observed in this mineral group.

1. Introduction

Schwertmannite [$Fe_8O_8(OH)_6SO_4$] and ferrihydrite [$5Fe_2O_3{\cdot}9H_2O$] are poorly crystalline minerals formed by the rapid oxidation of Fe in surface and ground waters. Ferrihydrite occurs in many environments under circumneutral to alkaline conditions, whereas schwertmannite forms primarily from acid sulfate waters in the pH range 2.8–4. Both minerals are meta-stable and are commonly associated with goethite [α-FeOOH]. Schwertmannite may also co-exist with jarosite [$KFe_3(SO_4)_2(OH)_6$], which forms under more acidic (pH < 3.0) conditions.

The properties of ferrihydrite have been widely studied, whereas schwertmannite was only recently recognized by the Commission on New Minerals and Mineral Names (Bigham et al., 1994). Since its original description, schwertmannite has been identified at several

* Corresponding author. Fax.: +41-21-6924315.
E-mail address: bernhard.dold@cam.unil.ch (B. Dold).
[1] Present address: CAM, Earth Sciences Department (BFSH 2), University of Lausanne, 1015 Lausanne, Switzerland.

0883-2927/03/$ - see front matter © 2003 Elsevier Ltd. All rights reserved.
doi:10.1016/S0883-2927(03)00015-5

locations around the world, especially in areas impacted by mining (Schwertmann et al., 1995; Bigham et al., 1996a; Childs et al., 1998; Yu et al., 1999; Dold and Fontboté, 2002). Dold et al. (1999) and Dold and Fontboté (2001) demonstrated its presence for the first time in the unsaturated oxidation zone of mine tailings from two porphyry copper mines in Chile. This finding showed that schwertmannite may be a common weathering product in oxidation and precipitation zones where ferrihydrite, goethite, and jarosite have previously been recognized (Jambor, 1994; Ribet et al., 1995).

Schwertmannite and ferrihydrite are of interest because of their high specific surface areas and chemical reactivity. Both minerals are thought to play important roles in the adsorption or incorporation of trace elements that may be mobilized in soils, stream sediments, and mine tailings impoundments (Davis and Kent, 1990; Webster et al., 1998; Dold et al., 1999; Dold and Fontboté, 2001; Swedlund and Webster, 2001). The stability fields of schwertmannite and ferrihydrite are pε-pH controlled so that these two minerals may play different roles in metal retention in mine tailings or acid rock drainage systems (Dold and Fontboté, 2001).

The broad, low-intensity X-ray diffraction (XRD) peaks of schwertmannite and ferrihydrite complicate their routine identification, especially if present in low concentration. For many years, a common method of detecting and "quantifying" ferrihydrite in soils has been through selective dissolution with 0.2 M NH_4-oxalate at pH 3 in the dark (Schwertmann, 1964). Schwertmann et al. (1982) coupled acid NH_4-oxalate extraction with the method of differential X-ray diffraction (DXRD) (Schulze, 1981) and found that the XRD detection limit for ferrihydrite in multi-phase samples was improved by a factor of 6 or 7 times. Numerous variations of experimental protocol have been proposed, but Cornell and Schwertmann (1996) have suggested a 2–4 h reaction time for complete ferrihydrite extraction. Fischer (1976) investigated the dissolution kinetics of 2-line ferrihydrite and observed a slower dissolution rate for slowly precipitated as compared to rapidly precipitated samples. Ferrihydrite with better crystallinity or Si-bearing ferrihydrite samples also dissolved more slowly. The dissolution kinetics of 6-line ferrihydrites have not been investigated to date. Nor have ferrihydrites associated with mine waters been systematically evaluated.

Bigham et al. (1990) observed that schwertmannite samples were soluble in pH 3 NH4-oxalate and reported that complete dissolution could be achieved within 15 min in the dark. These authors also studied the dissolution kinetics of two natural schwertmannite samples with 0.1 M HCl. A sigmoidal shape of the Fe dissolution curve was interpreted as a change in particle morphology (e.g., dissolution cavities, break up of aggregates), and a fast release of SO_4^{2-} detected at the beginning of the dissolution process was interpreted as a "burst" of surface adsorbed SO_4^{2-}. Differences in bulk dissolution rates between the two samples were interpreted as arising from differences in particle morphology.

Schwertmannites and ferrihydrites may form as co-associated mineral phases in mine-impacted environments (Bigham et al., 1996b). The primary objectives of the present study were to (1) investigate the possibility of discriminating between schwertmannite and ferrihydrite on the basis of dissolution kinetics in acid NH_4-oxalate, (2) determine if the method of DXRD can facilitate the detection of schwertmannite in natural mine tailings and sediments where previous studies have demonstrated the value of sequential extractions for evaluating the role of secondary minerals in trace element retention (Dold, 2001; Dold and Fontboté, 2001, 2002).

2. Samples and methods

Five specimens of schwertmannite, three of 2-line ferrihydrite, and one of 6-line ferrihydrite were used for dissolution studies. Samples MS1, MS3, PR1, PR2, and BT3 were ochreous precipitates collected from coal-mine drainage in Ohio, USA (Winland et al., 1991; Bigham et al., 1996a). Of these, samples MS1 and BT3 were formed at pH 5–7.5 and were composed mainly of ferrihydrite; whereas MS3, PR1 and PR2 were formed under more acidic conditions and contained schwertmannite mixed with goethite and detrital minerals (Table 1). Sample AS3/016 was also a natural sample and was hand-picked from schwertmannite-containing streaks in the oxidation zone of the Piuquenes tailings

Table 1
Description of the natural samples used for the dissolution kinetic tests and the pH of the source waters. Fe and SO_4 of HCl-soluble fraction

Sample	Mineralogy	pH	Fe (mol/kg)	SO_4 (mol/kg)	Fe/S mol ratio
MS3	Sh, Gt(t)	2.8	9.0	2.05	4.4
PR1	Sh, Gt(t)	3.2	8.9	1.70	5.2
PR2	Sh, Gt(t)	2.8	10.3	1.83	5.6
MS1	2L-Fh	5.8	7.0	0.71	9.9
BT3	2L-Fh	7.5	9.4	0.17	55.3
AS3/016	Sh, Jt	3.16[a]	0.099	0.020	4.9

Modified after Winland et al. (1991) and Bigham et al. (1996a). Data for AS3/016 are from this study. MS1 was determined to be a 2-line ferrihydrite based on the results of this study (Dold, 1999) which is in contrast with the original description as a ferrihydrite-schwertmannite mixture by Bigham et al. (1996a).Fh = Ferrihydrite, 2L = two line, Sh = schwertmannite, Gt = goethite, Jt = jarosite, (t) = trace.

[a] In situ pH with a special glass electrode.

impoundments at the La Andina porphyry copper deposit, Central Chile (Dold, 1999; Dold et al., 1999; Dold and Fontboté, 2001). The secondary mineralogy of this sample was dominated by jarosite and a vermiculite-type mixed-layer mineral (Dold and Fontboté, 2001). Synthetic schwertmannite (sample Sh4) was prepared using the method of Bigham et al. (1990). A 2-line (2L-Fh) and a 6-line ferrihydrite (6L-Fh) were prepared using the methods described by Schwertmann and Cornell (1991). The synthetic samples were kindly provided by Professor U. Schwertmann, Lehrstuhl für Bodenkunde, Technische Universität München, Germany.

All samples were characterized by powder XRD using a 3020 Philips diffractometer with CuK_α ($\lambda = 1.54056$ Å) radiation (40 kV, 30 mA) and a diffracted-beam monochromator. Scans were collected using a 0.05° 2θ step interval and 20 s counting time per step. Differential X-ray diffraction was performed on the schwertmannite-containing samples following selective dissolution of schwertmannite with acid ammonium oxalate (see below) using the general methods described by Schulze (1981, 1994).

The samples were subjected to dissolution at room temperature in the absence of light with freshly prepared 0.2 M NH_4-oxalate solution brought to pH 3.0 with 0.2 M oxalic acid (Schwertmann, 1964). The dissolution-time curves were developed by shaking 125 mg of sample in 250 ml oxalate solution and taking 10 ml subsamples with syringes at 3, 6, 9, 12, 15, 20, 30, 45, 60, 120 min. The solutions were immediately filtered with 0.2 μm Teflon inline filters, and dissolved Fe and S were measured in triplicate by inductively coupled plasma-atomic emission spectroscopy (ICP-AES). To calculate the percentage of Fe dissolved at any given time, the synthetic specimens were completely dissolved in NH_4-oxalate by exposure to light for 24 h. Goethite was present as a minor phase in most of the natural samples. Because of the low but significant solubility of goethite in pH 3 NH_4-oxalate under UV light, it was not possible to obtain 100% dissolution values for the natural schwertmannite/ferrihydrite samples by exposure to light. These samples reached a dissolution plateau after 60 min, so it was assumed that 100% of the natural schwertmannite/ferrihydrite was dissolved after 120 min extraction in the dark. The dissolution curves were modeled with rate equations (Table 2) as outlined by Cornell and Schwertmann (1996), and curves were calculated to achieve best fits by iteration.

Two subsamples of MS3 and PR1 were reacted with acid NH_4-oxalate and the reaction was quenched at predetermined times (12 and 35 min for MS3; 7 and 30 min for PR1) by filtering with a 0.45 μm Na-acetate filter. The air-dried residues were then studied with a scanning electron microscope (SEM) to evaluate changes in particle morphology and to test the modeled geometric dissolution of spherical schwertmannite.

3. Results and discussion

3.1. X-ray diffraction results

X-ray diffraction analyses of the synthetic schwertmannite and ferrihydrite specimens (Sh4, 2L-Fh, 6L-Fh) gave results (Fig. 1) consistent with those reported elsewhere (Cornell and Schwertmann, 1996) and showed no evidence of other phases. The natural ferrihydrites (BT3 and MS1) were similar to the synthetic 2-line material, and contained only trace amounts of impurities. By contrast, the natural schwertmannite samples included significant amounts of goethite, quartz, and non-oxide phases such as phyllosilicates, and jarosite. Schwertmannite in the Chilean tailings sample could only be identified by DXRD due to the high content of other phases (Fig. 2a). Scanning electron micrographs of this sample showed web-like structures (Fig. 2b) that were believed to be the schwertmannite components.

DXRD also facilitated the identification of schwertmannite in the Ohio mine drainage sediments (Fig. 3). Sample MS3 was mostly a 3-phase material composed of schwertmannite, goethite, and quartz. A DXRD performed after 30 min treatment with acid NH_4- oxalate in the dark and using an intensity correction factor of $k = 0.25$ showed that schwertmannite and a small amount of goethite were removed by this extraction (Fig. 3a). A similar leaching of samples PR1 and PR2 dissolved even greater amounts of goethite. For these samples, a 15-min extraction removed only schwert-

Table 2
Rate equations used for modeling the dissolution kinetics curves (from Cornell and Schwertmann, 1996)

Equation	Type	Physical meaning	
$(1-\alpha) = e^{-kt}$	Deceleratory	First order equation	(1)
$\alpha^2 = kt$	Deceleratory	One-dimensional diffusion	(2)
$1-(1-\alpha)^{1/3} = kt$	Geometric	Phase boundary controlled for a contracting sphere (cube root)	(3)
$1-\alpha = e^{-(kt)a}$	Variable	No physical meaning (Kabai equation)	(4)

α = Fraction dissolved at time t; a = constant; t = time; k = rate constant.

mannite from PR1 but still dissolved significant amounts of goethite from PR2 (Fig. 3b and c). These results indicate the importance of dissolution kinetics for achieving optimal mineral determinations by DXRD. They also suggest that significant differences in oxalate solubility exist among natural schwertmannites.

3.2. Dissolution of schwertmannite

The dissolution reaction was 94% complete for all schwertmannite samples after 60 min contact with acid NH_4-oxalate; however, the shapes of the dissolution curves could be divided into two groups (Fig. 4a). In one case (Sh4 and MS3), the dissolution was initially

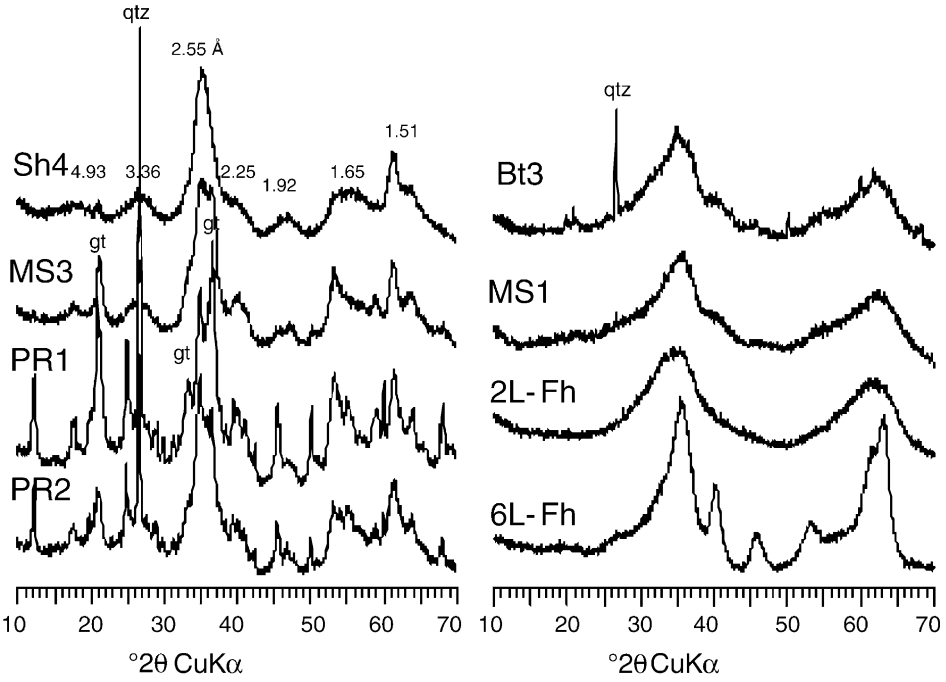

Fig. 1. X-ray powder diffraction patterns of the studied samples. Descriptive details of the natural samples MS3, PR1, PR2, BT3, MS1 are given in Table 1. Sh4, 2L-Fh, and 6L-Fh are synthetic samples. Abbreviations: gt = goethite, qtz = quartz.

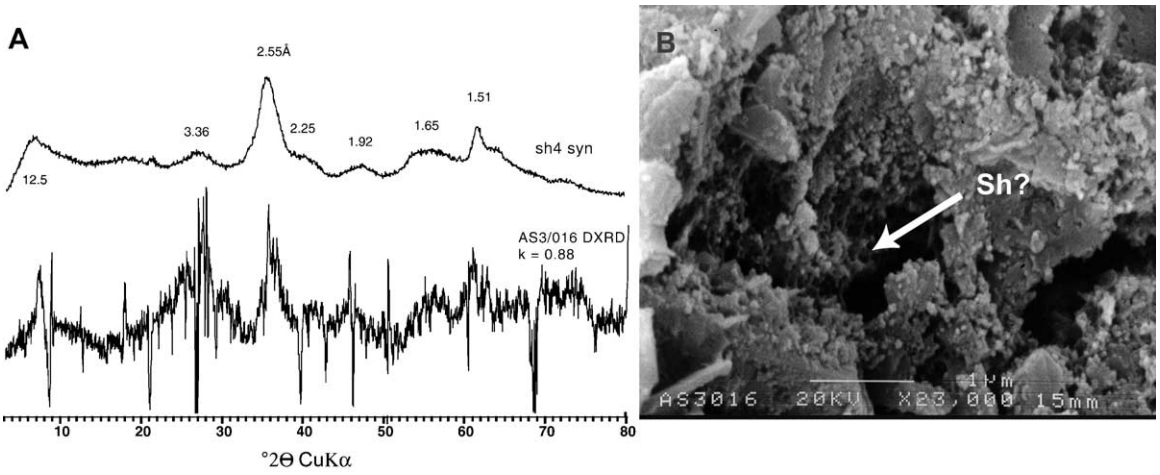

Fig. 2. (A) Differential X-ray powder diffraction (DXRD) pattern of sample AS3/016 after 15 min treatment with acid NH_4-oxalate in the dark (intensity correction $k = 0.88$), showing schwertmannite. X-ray powder diffraction (XRD) pattern of the synthetic schwertmannite samples Sh 4 is shown above. (B) SEM microphotograph of Fe-rich web-like structures in the sample AS3/016, possibly representing schwertmannite (compare to Fig. 6).

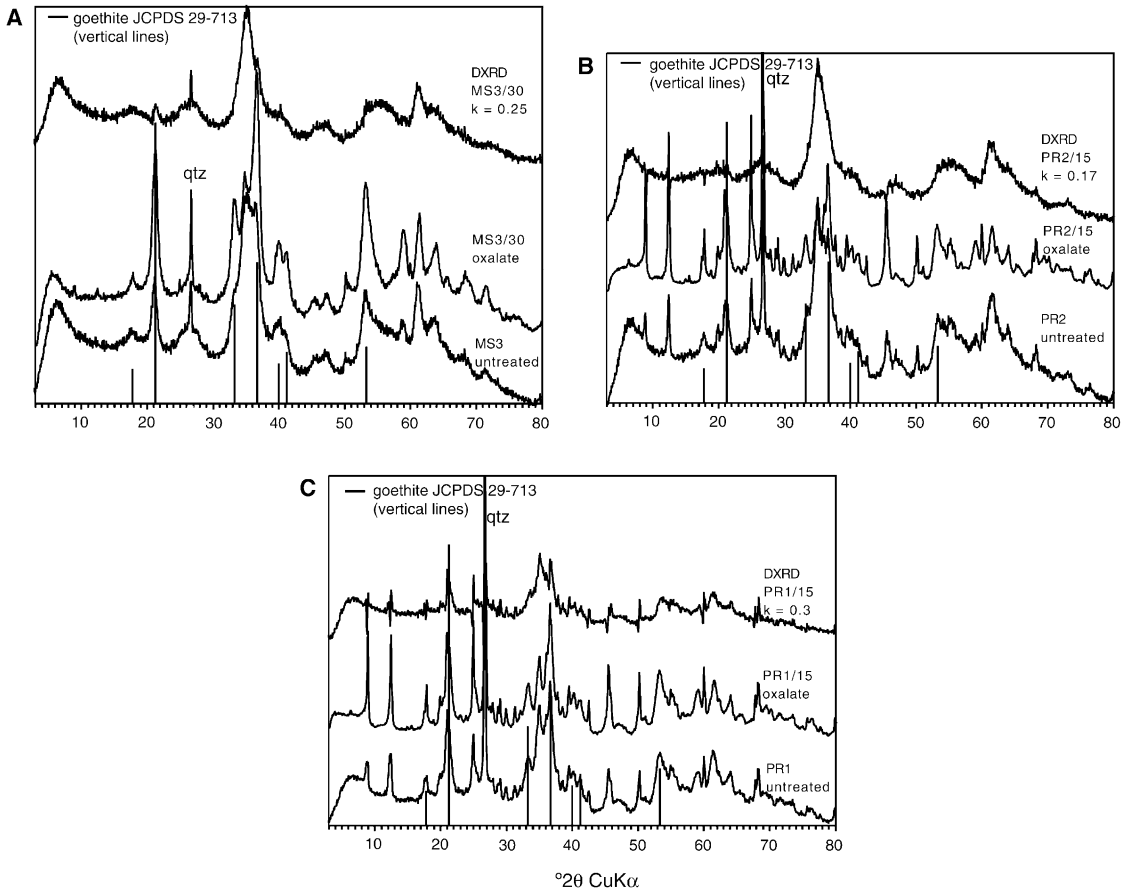

Fig. 3. Differential X-ray diffraction (DXRD) patterns of (a) MS3, (b) PR2, and (c) PR1 after 30, 15, and 15 min treatment with NH_4-oxalate in the dark (intensity correction $k = 0.25$, 0.17, and 0.3, respectively) on comparing of their XRD patterns before and after treatment. In the case of MS3 and PR2 mainly schwertmannite was dissolved in the applied dissolution time. Only very small amounts of dissolved goethite can be detected in these samples (compare main peak position of goethite JCPDS 29-713 patterns). In contrast, the DXRD of the sample PR1 shows dissolution of important amounts of goethite after 15 min dissolution time.

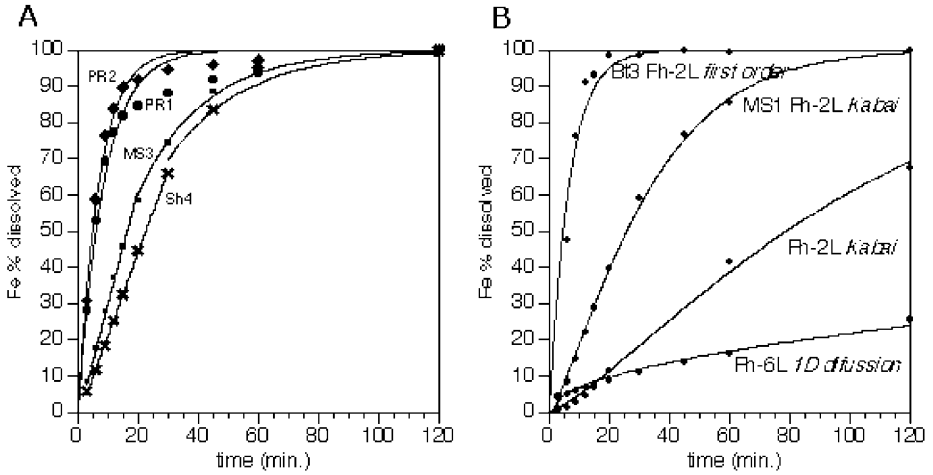

Fig. 4. (a) dissolution kinetic values (dots) and modeled curves of the schwertmannite samples MS3, Sh4, PR1, and PR2. Note that after 20 min in the case of MS3 and 30 min in the case of Sh4 the used model changes from contracting sphere to dissolution as a function of the remaining surface. (b) dissolution kinetic results of the ferrihydrite samples Bt3, MS1, 2L-Fh, and 6L-Fh.

linear over time but became exponential after 20–30 min (Fig. 5a and b). SEM images showed that both Sh4 and MS3 were composed of spherical particles with spicules resembling sea-urchins (Fig. 6 A and D1). Accordingly, the linear portion of the dissolution curve could best be modeled by a geometric expression indicating that the phase boundary was controlled by a contracting sphere [Table 2, Eq. (3)]. The exponential segment was best described by a first order equation [Table 2, Eq. (1)] which indicated that at any time, t, the dissolution rate was a function of the remaining surface (Cornell and Schwertmann, 1996). The change in the curve shape is thought to reflect the moment at which the spherical geometry of schwertmannite collapses, and the residual schwertmannite fragments dissolve as a function of their remaining surface area. The soluble Fe/S mole ratios initially increased with time (Table 3, Fig. 5a and b) indicating that most of the SO_4 was located at or near the particle surfaces. After 20 to 30 min, the ratios stabilized and were in the range of 4.6–8.0 that is reported to be typical for schwertmannite (Bigham et al., 1996a,b).

The second group of schwertmannite samples (PR1, PR2, and AS3/016) showed slightly faster dissolution with exponential behavior throughout and could be modeled entirely by a first order equation. Characterization of the particle shape by SEM showed that the schwertmannite in these samples had web-like, filigree morphologies (Fig. 2B; Fig. 6B and E1). After 12 min (in the case of PR1) to 15 min (in the case of PR2), the dissolution rate slowed down. Replotting the data using a logarithmic scale (Fig. 7) confirmed a break at these

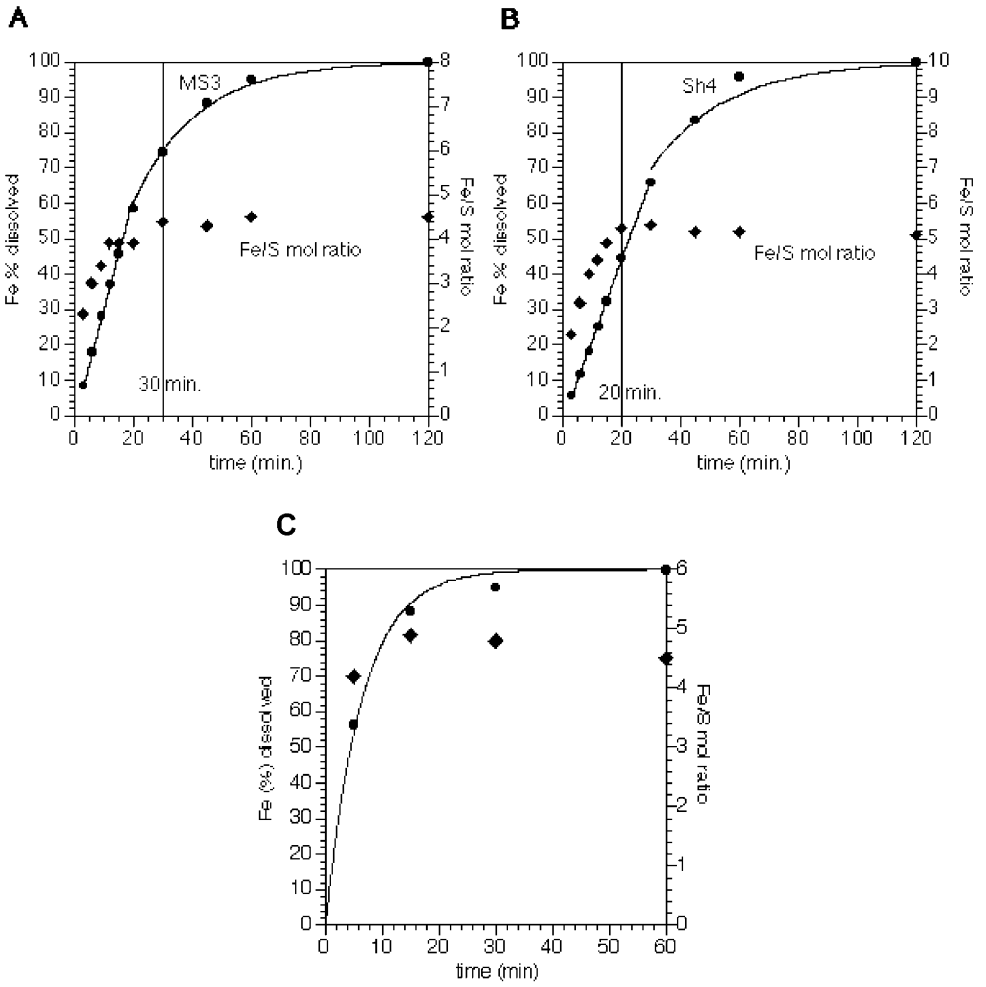

Fig. 5. (a) Dissolution curve of schwertmannite samples MS3 and (b) Sh4. Round dots are measured Fe-values, diamonds represent Fe/S mole ratio values. The line is modeled. (c) Dissolution kinetics and Fe/S mole ratios of the mine tailings sample AS3/016 (Piuquenes/ La Andina). For discussion see text.

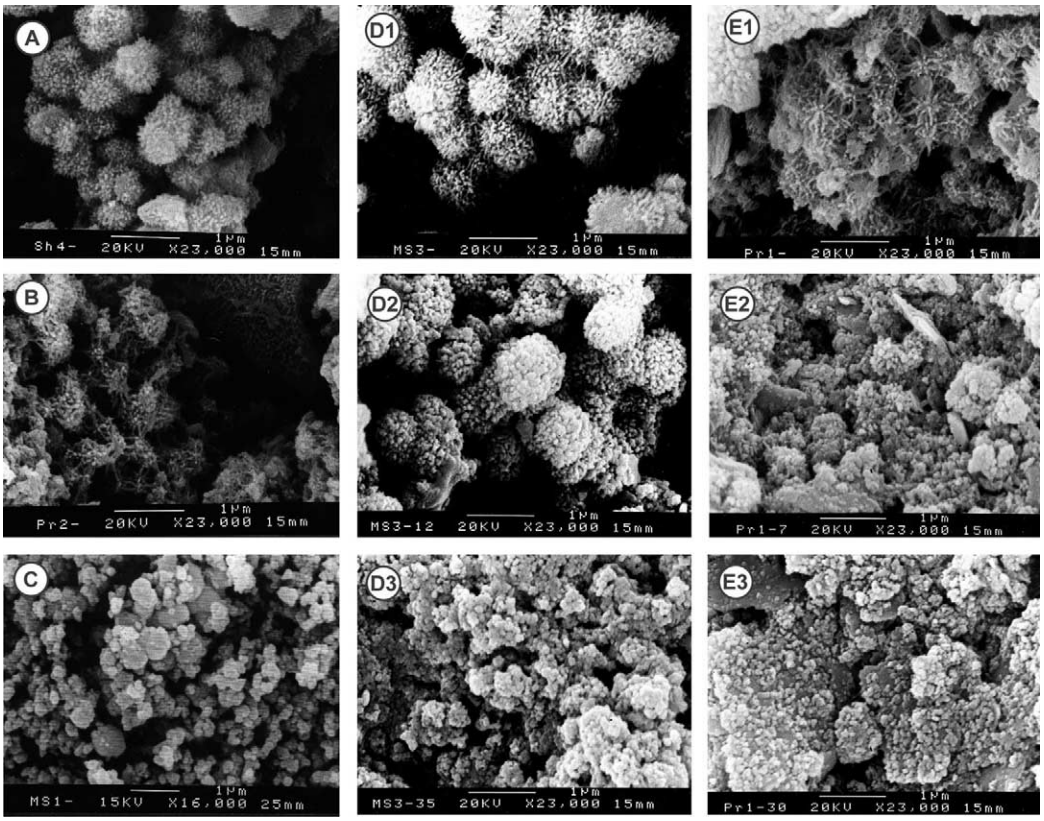

Fig. 6. SEM images of the schwertmannite samples Sh4(a), PR2(b), and ferrihydrite samples MS1(c) for the dissolution kinetic curves shown in Fig. 4. MS3 (D1) and Sh4, which were modeled by a contracting sphere show the typical spherical particles of schwertmannite with spicules reminiscent of sea-urchins. In contrast, the faster dissolving schwertmannite phases PR1(E1) and PR2 (b) show web-like, filigree structures. MS1 shows very fine irregularly shaped particles. MS1 does not show any features of schwertmannite structures so that it was classified as a 2-line ferrihydrite. **Fig. D1-3 and E1-3:** SEM images of samples MS3 and PR1. Center column (D1-3), from top to bottom: MS3 after 0, 12, and 35 min acid NH_4-oxalate dissolution. Right column (E1-3), from top to bottom: PR1 after 0, 7, and 30 min dissolution. MS3 after 12 min dissolution still shows spherical shape as expected from the modeling of the dissolution results, while, after 35 min, only fine irregular particles are left, which dissolve as a function of their surface. PR1 shows in the first shape control (after 7 min) only very fine irregular residual particles. Modeling of the dissolution kinetic tests suggests that they dissolve as a function of their surface.

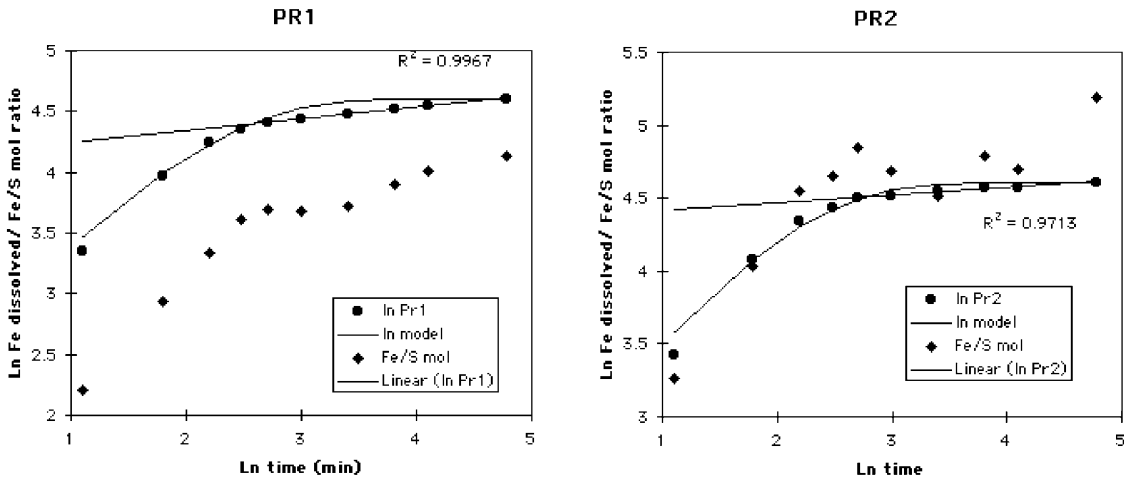

Fig. 7. PR1 and PR2 dissolution curves and Fe/S mole ratios on logarithm scales. For discussion see text.

Table 3
Data of the dissolution tests. Mole ratio refers to concentrations in solution

Time (min)	PR1 (Sh) Fe (% dis)	PR1 (Sh) Fe/S mole	PR2 (Sh) Fe (% diss)	PR2 (Sh) Fe/S mole	MS3 (Sh) Fe (% diss)	MS3 (Sh) Fe/S mole	Sh4 (Sh) Fe (% diss)	Sh4 (Sh) Fe/S mole	AS3/016 (Sh) Fe/S mole	Bt3 (2L-Fh) Fe (% diss)	2L-Fh syn Fe (% diss)	6L-Fh syn Fe (% diss)	MS1 (2L-Fh) Fe (% diss)
3	28.4	2.2	30.8	3.3	8.7	2.3	5.8	2.3		–	1.0	4.2	4.7
6	53.1	2.9	58.8	4.0	18.0	3.0	11.9	3.2	4.2	47.6	1.5	5.1	8.6
9	69.5	3.3	76.4	4.6	28.2	3.4	18.3	4.0		76.6	2.7	6.1	14.7
12	77.4	3.6	83.8	4.6	37.3	3.9	25.3	4.4		91.3	4.6	6.9	22.2
15	82.0	3.7	89.8	4.8	45.9	3.9	32.5	4.9	4.9	93.3	6.9	7.9	29.0
20	84.9	3.7	91.8	4.7	58.6	3.9	44.7	5.3		98.6	11.7	9.1	39.9
30	88.2	3.7	94.7	4.5	74.6	4.4	66.0	5.4	4.8	98.7	–	11.1	59.2
45	92.0	3.9	96.2	4.8	88.6	4.3	83.7	5.2		100.0	–	13.9	77.0
60	94.0	4.0	97.2	4.7	95.1	4.5	96.0	5.2	4.5	99.8	41.8	16.4	85.8
120	100.0	4.1	100.0	5.2	100.0	4.5	100.0	5.1		100.0	67.5	25.7	100.0

Abbreviations: Sh = schwertmannite, 2L-Fh = 2-line ferrihydrite, 6L-Fh = 6-line ferrihydrite, % diss = % dissolved, – = no data.

times that also corresponded to the points at which the soluble Fe/S ratios reached nearly constant values (see Table 2). The lower Fe/S mole ratios observed at the beginning of the schwertmannite dissolution indicated a higher SO_4^{2-} release compared to Fe, possibly due to surface adsorbed SO_4^{2-}, as reported by Bigham et al. (1990). The point of change to stable SO_4^{2-} release corresponded to lower dissolution rates, possibly because of a stabilizing effect on the crystal structure by SO_4^{2-}.

In the case of sample AS3/016, Fe dissolution was also rapid (56, 88.4, 95, and 100% after 5, 15, 30, and 60 min, respectively; Fig. 5c) and the data were best fit by a first order dissolution equation. The Fe/S mole ratio reached its maximum value of 4.9 after 15 min attack and subsequently decreased to 4.5 after 60 min. DXRD data (Fig. 2a) indicated that after 15 min mainly schwertmannite went into solution. A DXRD analysis after 60 min (data not shown), demonstrated that an easily soluble component of secondary jarosite had also dissolved (primary, i.e. supergene jarosite shows usually lower solubility and does not dissolve in NH_4-oxalate in darkness), explaining the decrease of the Fe/S mole ratio (Fig. 5c). Application of this method to tailings samples from elsewhere in the oxidation zone and at other locations in the Chilean tailings also revealed significant dissolution of secondary jarosite after 1h, as indicated by increased K concentrations in the leach (Table 4) (Dold, 1999; Dold and Fontboté, 2001).

To correlate possible changes in schwertmannite particle morphology (spherical or web-like) with dissolution rate, aliquots of MS3 and PR1 were examined by SEM following partial dissolution. Particles of sample MS3 retained a spherical form after 12 min reaction, whereas only granular particles remained after 35 min (Fig. 6, D1–D3). This result is consistent with a model based on a contracting sphere for the beginning of the dissolution curve and with a subsequent change to a first order equation when the spherical structure collapses. In contrast, sample PR1 did not show any schwertmannite morphology remaining after even 7 min, supporting the use of a dissolution model based only on the surface of the residual particles (Fig. 6, E1-E3).

It is not known what conditions lead to the different morphological varieties of schwertmannite. Explanations of the differences in mineral shape and dissolution kinetics could be SO_4^{2-} contents (Bigham et al., 1990), hydrolysis kinetics at the time of mineral precipitation, or oxyanion substitution in the schwertmannite (Waychunas et al., 1995; Barham, 1997). At least for samples MS3 and PR1, arsenate substitution did not seem to be responsible for the different mineral shapes and associated dissolution kinetics, as in both cases As contents were <1 μg l^{-1} (detection limit) in the leach solutions. Also, the Fe/S mole ratios of the schwertmannite samples did not provide any clear evidence of SO_4^{2-} control on dissolution kinetics or shape.

Table 4
K concentrations in the 1 h 0.2 M NH_4-oxalate, pH 3, darkness leach of sequential extractions from samples from the oxidation (Ox. Zone) and primary zone (Pry. Zone) from the studied porphyry copper tailings Piuquenes (La Andina) and Cauquenes (El Teniente), Chile (data from Dold and Fontboté, 2001)

Samples from Piuquenes/Andina	K (%) *in* *NH_4-oxalate leach*	Samples from Cauquenes/Teniente	K (%) *in* *NH_4-oxalate leach*
Ox. Zone A2/020	0.24	Ox. Zone T4/040	0.07
Ox. Zone A2/050	0.19	Ox. Zone T4/153	0.07
Pry. Zone A2/100	0.01	Pry. Zone T4/490	0.01
Pry. Zone A2/900	0.02	Pry. Zone T4/490	0.01

3.3. Dissolution of ferrihydrite

Dissolution curves of ferrihydrite (Fig. 4b) showed more variability than those of schwertmannite, and the natural ferrihydrites clearly dissolved faster than synthetic ones. The latter difference is possibly due to microbiological interactions during formation of the natural ferrihydrites, as proposed by Fischer (1976). The dissolution of sample BT3 was very fast (> 90% in 15 min) and could be modeled by a first order equation. In contrast, the dissolution curves of samples MS1 and 2L-Fh showed a more sigmoidal shape (Fig. 4b). This behavior presumably reflected a change in particle morphology (dissolution cavities, break up of aggregates, etc.) during the initial stage of dissolution (Schwertmann, 1984). Both curves could be modeled with the Kabai equation [Table 2, Eq. (4)]. This equation provides a flexible way of summarizing experimental data, but it is not based on any fundamental conceptual model of the dissolution process and therefore has no physical meaning (Cornell and Schwertmann, 1996). The dissolution curve of the 6-line synthetic ferrihydrite (6L-Fh) could best be modeled with a one-dimensional diffusion model [Table 2, Eq. (2)], suggesting that slow diffusion of the chelate-former oxalate into the ferrihydrite surface controls the dissolution kinetics.

4. Conclusions

The identification of low crystallinity Fe(III) minerals such as ferrihydrite and schwertmannite as monomineralic samples is easily achieved by XRD (Fig. 1). To detect these minerals as minor components of multiphase samples containing well-crystallized minerals (quartz, feldspar, micas, carbonates, Fe-oxides, sulfides, and sulfates) requires more sophisticated approaches. DXRD is perhaps the best technique under these circumstances, but it requires at least a general knowledge of the dissolution kinetics. DXRD analyses of mine drainage precipitates containing both schwertmannite and goethite showed that only 15 min contact time with acid 0.2 M NH_4-oxalate was sufficient to dissolve significant amounts of goethite from some samples (Fig. 3). Likewise, the extraction of samples from the oxidation zone of sulfidic mine tailings revealed that some secondary jarosite was dissolved, although at a slower rate than schwertmannite and ferrihydrite. It must also be taken into account that in the presence of Fe(II) containing minerals (e.g., siderite, magnetite), the dissolution rate of other Fe(III) oxides (goethite, hematite, etc.) may be enhanced (Suter et al. 1988, 1991).

The adoption of a single extraction time using acid NH_4-oxalate can not be expected to yield perfect results, but it has practical advantages when processing large numbers of samples. The results summarized in Table 3 suggest that to attain almost complete dissolution of schwertmannite and 2-line ferrihydrite in mine spoils and sediments (with minimal attack of associated mineral phases), a 60 min reaction with 0.2 M NH_4-oxalate at pH 3 in the dark should be chosen. Under these conditions, > 94% schwertmannite and > 85% 2-line ferrihydrite were dissolved while minimizing the removal of other Fe-bearing phases such as jarosite and goethite. If only schwertmannite is of interest (e.g., determination by DXRD), a 15 min attack should be used to increase selectivity. The results of this study also show that it is not possible to discriminate between schwertmannite and ferrihydrite on the basis of their dissolution rates in acid NH_4-oxalate. Natural 2-line ferrihydrite dissolves at the same rate as schwertmannite, while synthetic 2-line ferrihydrite dissolves slower (41.8% after 60 min). Synthetic 6-line ferrihydrite shows a very slow dissolution rate (16.4% after 60 min) due to its higher structural order.

Dissolution curves, examinations of particle morphology by SEM, and Fe/S mole ratios of the dissolved fractions indicate that two different schwertmannite shapes (spherical and web-like) with different dissolution kinetics can be distinguished. The collapse of spherical shaped (sea-urchin) schwertmannite aggregates seems to control the dissolution kinetics. In the case of web-like schwertmannite, SO_4^{2-} may have a dominant effect on the stability of the structure. Further studies are needed to understand and define the differences in observed schwertmannite morphology.

Acknowledgements

I would like to thank to J.M. Bigham and U. Schwertmann for supplying the samples and helpful comments and corrections of the manuscript. I am also grateful to L. Fontboté and W. Wildi for their support and helpful suggestions, and B.M. Thompson and C.N. Alpers for critically reading the manuscript. I thank H-R. Pfeifer and his group for the facilities and discussions in the laboratory of the Centre de Analyse de Mineralogie, Université de Lausanne. Thanks to J.-P. Dubois from the Soil Science Institute of the EPFL, Lausanne for the ICP analysis and R. Martini from the Geological Department, University of Geneva for the patient SEM work. The project is supported by the German Academic Exchange Service (DAAD) and the Swiss National Science Foundation project No. 21-50778.97.

References

Barham, R.J., 1997. Schwertmannite: a unique mineral, contains a replaceable ligand, transforms to jarosites, hematites, and/or basic iron sulfates. J. Mater. Res. 12, 2751–2758.

Bigham, J.M., Schwertmann, U., Carlson, L., Murad, E., 1990. A poorly crystallized oxyhydroxysulfate of iron formed by bacterial oxidation of Fe(II) in acid mine waters. Geochim. Cosmochim. Acta 54, 2743–2758.

Bigham, J.M., Carlson, L., Murad, E., 1994. Schwertmannite, a new iron oxyhydroxy-sulphate from Pyhäsalmi, Finland, and other localities. Mineral. Mag. 58, 641–648.

Bigham, J.M., Schwertmann, U., Traina, S.J., Winland, R.L., Wolf, M., 1996a. Schwertmannite and the chemical modeling of iron in acid sulfate waters. Geochim. Cosmochim. Acta 60, 185–195.

Bigham, J.M., Schwertmann, U., Pfab, G., 1996b. Influence of pH on mineral speciation in a bioreactor simulating acid mine drainage. Appl. Geochem. 11, 845–849.

Childs, C.W., Inoue, K., Mizota, C., 1998. Natural and anthropogenetic schwertmannites from Towada-Hachimantai National Park, Honshu, Japan. Chem. Geol. 144, 81–86.

Cornell, R.M., Schwertmann, U., 1996. The Iron Oxides. VCH Verlagsgesellschaft mbH, Weinheim.

Davis, J.A., Kent, D.B., 1990. Surface complexation modeling in aqueous geochemistry. In: Hochella, M.F., White, A.F. (Eds.), Reviews in Mineralogy, Mineral. Soc. Am. 23, 177–260.

Dold, B., 1999. Mineralogical and Geochemical Changes of Copper Flotation Tailings in Relation to their Original Composition and Climatic Setting—Implications for Acid Mine Drainage and Element Mobility. Terre & Environnement, Vol. 18, Geneva.

Dold, B., 2001. A 7-step sequential extraction for geochemical studies of copper sulfide mine waste. Securing the Future. International Conference on Mining and the Environment, Skellefteå, Sweden, pp. 158–170.

Dold, B., Fontboté, L., 2001. Element cycling and secondary mineralogy in porphyry copper tailings as a function of climate, primary mineralogy and mineral processing. Special Issue: Geochemical studies of mining and the environment. J. Geochem. Explor. 74, 3–55.

Dold, B., Fontboté, L., 2002. A mineralogical and geochemical study of element mobility in sulfide mine tailings of the Fe-oxide Cu–Au deposits from the Punta del Cobre district, northern Chile. Chem. Geol. 189, 135–163.

Dold, B., Fontboté, L., Wildi, W., 1999. Detection and distribution of ferric oxyhydroxides and oxyhydroxide sulfates in sulfide mine tailings; their importance to selective metal retention and acid production. Mine, Water and Environment; Sevilla 2, 525–526.

Fischer, W.R., 1976. Differenzierung oxalatlösllicher Eisenoxide. Z. Pflanzen. Bodenkunde 139, 641–646.

Jambor, J.L., 1994. Mineralogy of sulfide-rich tailings and their oxidation products. In: Jambor, J.L., Blowes, D.W. (Eds.), Short Course Handbook on Environmental Geochemistry of Sulfide Mine Waste, vol. 22. Mineralogical Association of Canada, Nepean, pp. 59–102.

Ribet, I., Ptacek, C.J., Blowes, D.W., Jambor, J.L., 1995. The potential for metal release by reductive dissolution of weathered mine tailings. J. Contam. Hydrol. 17, 239–273.

Schulze, D.G., 1981. Identification of soil iron oxide minerals by differential X-ray diffraction. Soil Sci. Soc. Am. J. 45, 437–440.

Schulze, D.G., 1994. Differential x-ray diffraction analysis of soil material. In Quantitative methods in soil mineralogy. SSSA Miscellaneous Publication 412–429.

Schwertmann, U., 1964. Differenzierung der Eisenoxide des Bodens durch Extraktion mit Ammoniumoxalat Lösung. Z. Pflanzen. Bodenkunde 105, 194–202.

Schwertmann, U., 1984. The influence of aluminium on iron oxides: IX. dissolution of Al-goethites in 6 M HCl. Clay Min. 19, 9–19.

Schwertmann, U., Cornell, R.M., 1991. Iron Oxides in the Laboratory. VCH Verlagsgesellschaft mbH, Weinheim.

Schwertmann, U., Schulze, D.G., Murad, E., 1982. Identification of ferrihydrite in soils by dissolution kinetics, differencial X-ray diffraction, and Mössbauer Spectroscopy. Soil Sci. Soc. Am. J. 46, 869–875.

Schwertmann, U., Bigham, J.M., Murad, E., 1995. The first occurrence of schwertmannite in a natural stream environment. Eur. J. Mineral. 7, 547–552.

Suter, D., Siffert, C., Sulberger, B., Stumm, W., 1988. Catalytic dissolution of iron(III)(hydr)oxides by oxalic acid in the presence of Fe(II). Naturwiss. 75, 571–573.

Suter, D., Banwart, S., Stumm, W., 1991. The dissolution of hydrous iron(III) oxides by reductive mechanisms. Langmuir 7, 809–813.

Swedlund, P.J., Webster, J.G., 2001. Cu and Zn ternary surface complex formation with SO4 on ferrihydrite and schwertmannite. Appl. Geochem. 16, 503–511.

Waychunas, G.A., Ning, Xu, Fuller, C.C., Davis, J.A., Bigham, J.M., 1995. XAS study of AsO_4^{3-} and SeO_4^{2-} substituted schwertmannites. Physica B 208, 209. 481-483.

Webster, J.G., Swedlund, P.J., Webster, K.S., 1998. Trace metal adsorption onto an acid mine drainage iron(III)oxyhydry sulfate. Environ. Sci. Technol. 32, 1362–1368.

Winland, R.L., Taina, S.J., Bigham, J.M., 1991. Chemical composition of ochreous precipitates from Ohio Coal Mine Drainage. J. Environ. Qual. 20, 452–460.

Yu, J.-Y., Heo, B., Choi, I.K., Cho, J.P., Chang, H.-W., 1999. Apparant solubilities of schwertmannite and ferrihydrite in natural stream waters polluted by mine drainage. Geochim. Cosmochim. Acta 63, 3407–3416.